



Journal of Agrometeorology

(A publication of Association of Agrometeorologists)

ISSN : 0972-1665 (print), 2583-2980 (online)

Vol. No. 27 (3) : 286-291 (September - 2025)

<https://doi.org/10.54386/jam.v27i3.2952>

<https://journal.agrimetassociation.org/index.php/jam>



Research Paper

Evaluating the use of extended range forecasts in DSSAT for predicting rice yield: A case study of Madhya Pradesh, India

MEHNAJ THARRANUM. A^{1*}, D. R. PATTANAİK², K. K. SINGH¹, SHESHAKUMAR GOROSHI¹ and S. K. MANIK³

¹Agromet Advisory Service Division, India Meteorological Department, New Delhi.

²Numerical Weather Prediction Division, India Meteorological Department, New Delhi.

³Hydrometeorology Division, India Meteorological Department, New Delhi.

*Corresponding author. Email: mtharranum@gmail.com

ABSTRACT

This study evaluates the potential of Extended Range Forecasts (ERFs) in improving rainfed rice yield simulations during three *kharif* seasons (2019–2021) using the DSSAT v4.8 model for Madhya Pradesh. Three weather datasets were evaluated: (1) observed weather, (2) observed + ERF + climatological normal and (3) observed + climatological normal. The ERF generated as weekly interval during the crop season with a total of 19 initial conditions (IC) were used for ERF dataset. The yields simulated using hybrid datasets (2 & 3) were related with those obtained with the observed weather data (1). Results indicated that integrating ERFs during the reproductive and ripening phases improves yield simulations, with the most notable improvements observed in 2021. However, benefits varied across seasons and growth phases. The findings highlight the potential of ERFs to enhance seasonal yield forecasts when applied strategically, particularly by bridging observed data and climatological normal during key crop phases.

Keywords: Extended range forecast (ERF), Rice, DSSAT, Vegetative phase, Reproductive phase, Ripening phase

Rice is a major staple crop in the Indian state of Madhya Pradesh, occupying approximately 3.41 million hectares during the 2022–23 cropping season. This represents 7.14% of India's total rice cultivation area and contributes 7.02 million tonnes—about 5.17% of the nation's total rice output—with an average productivity of 2057 kg ha⁻¹ (GoI, 2024). As of 2021–22, nearly 59.86% of the rice-growing area in the state was under irrigation, reinforcing Madhya Pradesh's status as one of the key rice-producing states in the country (GoI, 2024).

To facilitate agricultural planning and decision-making, the Government of India routinely releases crop production forecasts at different stages of the growing cycle, supplementing final yield statistics. As part of its agrometeorological services, the India Meteorological Department (IMD) provides three-stage yield forecasts—initial (F1) at planting, mid-season (F2), and pre-harvest (F3)—for twelve major crops, including rice. These forecasts are generated using a combination of statistical approaches and dynamic crop simulation models (IMD, 2014). The extended range

forecasts (ERFs) from IMD includes a 32-day forecast of maximum and minimum temperatures ($1^\circ \times 1^\circ$) and rainfall ($0.25^\circ \times 0.25^\circ$), derived from IMD's operational ERF system which is based on the CFSv2 coupled model from NCEP and was customised in Indian Institute of Tropical Meteorology (IITM) (Sahai *et al.*, 2013, 2015), Pune, before its implementation in IMD. The current ERF system integrates the fully coupled CFSv2 model with a GFS atmospheric model with bias-corrected SST (GFSbc), and utilizes an ensemble of 16 members (Pattanaik *et al.*, 2022). Chattopadhyay (2023) has demonstrated how the extended range weather forecast i.e., sub-seasonal forecast can be translated into agromet advisories for the farming communities to increase crop production in India. Crop simulation models that incorporate soil-crop-climate processes of plant growth and that are sensitive to climatic factors can be used to quantify impact of climate change on crop production (Singh, 2023). Harinarayanan *et al.*, (2022) had integrated the ERF forecast outputs in the DSSAT model for crop yield prediction for maize crop using in Erode district of Tamil Nadu.

Article info - DOI: <https://doi.org/10.54386/jam.v27i3.2952>

Received: 3 March 2025; Accepted: 24 July 2025; Published online : 1 September 2025

"This work is licensed under Creative Common Attribution-Non Commercial-ShareAlike 4.0 International (CC BY-NC-SA 4.0) © Author (s)"

This study aimed to assess the efficacy of ERFs in enhancing the accuracy of rice yield forecasts by appending weekly ERFs to observed weather data across key crop growth phases. The overarching objective was to evaluate the operational applicability of ERFs for agricultural forecasting in rainfed production systems of Central India.

MATERIALS AND METHODS

Study area and data

Ten districts of Madhya Pradesh representing a broad agroclimatic gradient spanning the eastern to western parts of the state were selected for evaluating the role of IMD's Extended Range Forecasts (ERFs) in rainfed rice yield prediction. The annual normal rainfall in these districts varies from 885.5 to 1445.1 mm with average rainfall of 1189.4 mm out of which about 90 per cent are received during the Southwest monsoon season (June to September) (Table 1).

Observed and extended range forecast (ERF) data

The daily observed weather data, including maximum and minimum temperatures at a $1^\circ \times 1^\circ$ spatial resolution and rainfall data at high-resolution gridded ($0.25^\circ \times 0.25^\circ$) dataset were obtained from the India Meteorological Department (IMD) for the period 2019–2021 (<https://imd pune.gov.in/lrfindex.php>). Climatological normal obtained from IMD for temperature ($1^\circ \times 1^\circ$) and rainfall ($0.25^\circ \times 0.25^\circ$) were also downscaled for each district to serve as a baseline for comparison. The extended range forecasts (ERFs) from IMD were utilized for 19 initial condition (IC) dates during each *kharif* season, with forecasts generated at weekly intervals (Table 2). Each IC date included a 32-day forecast of maximum and minimum temperatures ($1^\circ \times 1^\circ$) and rainfall ($0.25^\circ \times 0.25^\circ$), derived from IMD's operational ERF system. Forecasts are generated weekly using Wednesday ICs, with retrospective hindcasts also performed.

Model inputs and experimental planning

CERES-Rice module embedded in Decision Support System for Agrotechnology Transfer model, version 4.8 (DSSAT v4.8), was used to simulate the *kharif* rice yields over study locations. This module uses a minimum of readily available daily weather data, soil profile characteristics, crop management, and variety-specific genetic inputs. In Madhya Pradesh, 80% of rice is grown in rainfed fields. IR 36, a semi-dwarf rice variety, performed well in multi-location tests, and has become popular in areas where rainfall begins the 3rd week of June and continues through mid-September (Sahu, *et al.*, 1985). This crop variety was selected for the study, as its well documented genetic coefficients were available at Agromet Advisory Service Division, India Meteorological Department, New

Table 1: District wise normal rainfall of study area

S. No	District	Normal rainfall (mm)	
		Annual	SW monsoon
1	Betul	1081.3	950.4
2	Alirajpur	855.5	840.9
3	Raisen	1237.6	1143.2
4	Shahdol	1226.0	1063.1
5	Rewa	1143.1	1025.3
6	Mandla	1445.1	1289.3
7	Damoh	1170.4	1065.4
8	Panna	1182.9	1069.6
9	Singrauli	1175.6	1041.5
10	Dindori	1376.7	1230.0
Average		1189.4	1071.8

Delhi, for its use in DSSAT model run (Singh *et al.*, 2005). The 21 days' old seedlings were considered for date of transplanting on 10th July. Irrigation was not given, i.e., the crop was rainfed. Fertilization in the form of urea was fixed as split doses of nitrogen in the ratio of 50:25:25 (Basal dose: 25th day after planting: 45th day after planting).

Strategy of planning weather files

For each of the 10 districts, weather file was planned into 3 categories, comprising of three parameters viz. daily maximum temperature ($^\circ\text{C}$), daily minimum temperature ($^\circ\text{C}$) and daily rainfall (mm), of every year. These categories were: (i) OBS: Observed weather data (OBS); (ii) OBS+ERF+N: Observed weather data (OBS) with 32 days extended range forecast (ERF) data beginning from all 19 IC dates (Table 2) and climatological normal (N) and (iii) OBS+N: Combination of observed weather data (OBS) and climatological normal beginning (N) from all 19 IC dates.

The IC dates for the ERFs were selected starting from the second fortnight of June in each season to encompass the typical rice sowing period. The final IC date was chosen within the first fortnight of October. Utilizing ERF data in a moving weekly window enabled the evaluation of which forecast issuance date contributes most effectively to accurate yield prediction. These IC dates were further aligned with specific phenological stages of the rice crop to facilitate interpretation of results in the context of crop-weather interactions. Consequently, thirty-nine (39) distinct weather datasets were generated for each district, grouped into three categories. In the present study on rainfed rice, crop phenology analysis revealed that panicle initiation occurred between 46–48 days after planting (DAP) (24–26 August), heading (anthesis) between 83–88 DAP (30 September–6 October), and physiological maturity between 122–

Table 2: Initial condition (IC) dates used during three seasons

Season	June	July	August	September	October
2019	12, 19, 26	3, 10, 17, 24, 31	7, 14, 21, 28	4, 11, 18, 25	2, 9 and 16
2020	10, 17, 24	1, 8, 15, 22, 29	5, 12, 19, 26	2, 9, 16, 23, 30	7 and 14
2021	9, 16, 23, 30	7, 14, 21, 28	4, 11, 18, 25	1, 8, 15, 22, 29	6 and 13

Table 3: Seasonal rainfall (June–September) and number of rainy days over the study area

Year	Rainfall (mm)	Departure from normal (%)	Rainy days
2019	1359.3	+26.8	55.0
2020	1074.1	+0.2	48.8
2021	971.3	-9.4	45.2

129 DAP (9–16 November).

The relationship between stage-wise simulated yield was evaluated by computing correlations across three phenological phases which were ascertained by grouping of DSSAT-CERES defined rice model phases. These are: Vegetative phase comprising of emergence to end of juvenile phase (31–35 days), and end of juvenile to panicle initiation (30–44 days); Reproductive phase comprising of panicle initiation to end of leaf growth (33–40 days), and end of leaf growth to beginning of grain filling (6–9 days); Ripening phase from grain filling to physiological maturity (27–36 days).

The Pearson correlation coefficient (r) and Root Mean Square Error (RMSE) were computed for simulated yield derived from the observed weather (OBS) and compared against values obtained using the hybrid weather datasets of (OBS + ERF + N) and (OBS + N).

RESULTS AND DISCUSSION

The mean seasonal rainfall during the experimental years (2019–2021) in the study region showed that in 2019, the rainfall was 26.8% higher than the normal, while in 2021 it was 9.4% less than the normal. The number of rainy days varied between 45.2 to 55.0 days in different years (Table 3).

Correlations between yield predicted by different weather datasets

The correlation worked out between yield simulated using actual weather data (OBS) with those simulated hybrid data of ERF (OBS + ERF + N) and normal (OBS+N) using 19 initial conditions (IC) during three rice crop seasons (2019, 2020 and 2021) are presented in Fig. 1. During 2019 crop season, the correlation trends for simulated yields across all IC dates using ERF forecast datasets (OBS+ERF+N) and normal (OBS+N) presented in Fig. (1a), indicated a notable improvement in correlation from the IC date of 31 July 2019 onwards when ERF was incorporated, with the highest correlation ($r > 0.95^{**}$) observed around 7 August 2019. This suggests that the skill of ERF improves considerably during the latter part of the vegetative stage. During reproductive phase with four IC dates (28 August, 4, 11, and 18 September), the correlation coefficients were statistically significant ($r = 0.938$ to 0.960 ; $p < 0.01$). However, ERF-omitted datasets (OBS+N) consistently exhibited slightly higher correlation values ($r = 0.981$ to 0.990) than ERF-inclusive simulations. This suggests that in 2019, ERF inclusion did not provide added predictive benefit during the reproductive phase (Fig. 1a). During the ripening phase, the correlations for initial condition (IC) dates (25 September; 2, 9, and 16 October) with both ERF-inclusive and ERF-omitted simulations displayed statistically significant positive correlations with the

observed-weather-based yields (Fig. 1a).

During the vegetative phase of the 2020 crop season (IC dates from 10 June to 19 August), significant correlations ($p < 0.05$) between simulated yields from ERF-inclusive datasets and those based on observed weather were recorded on three IC dates 10 June ($r = 0.713$), 17 June ($r = 0.725^{*}$), and 1 July ($r = 0.751^{*}$). These results demonstrate the potential of early-season ERFs to capture spatial variability in rainfed rice yield with reasonable accuracy, despite higher RMSEs in mid-June and early July (Fig 1b). Across all IC dates, yield simulations using ERF-inclusive datasets consistently outperformed those generated with non-ERF datasets, both in terms of correlation with observed yield and RMSE values (Fig. 1b). This underscores the added value of ERFs in enhancing yield prediction accuracy during the vegetative growth phase of rainfed rice. Visual trends in (Fig. 1b) show variability and generally lower correlation during the reproductive phase, which may be attributable to atypical intra-seasonal climatic variability or reduced forecast skill during the 2020 monsoon. The sporadic correlation significance indicate that ERF had limited impact on enhancing reproductive-stage predictions in this season. These findings reinforce the potential of hybrid ERF datasets as effective inputs for mid-season yield forecasting and agrometeorological advisory services, particularly in rain-dependent rice-growing regions like central India.

Fig. (1c) illustrates the temporal trend in correlation coefficients between simulated rice yields derived from observed weather (OBS) and those generated using ERF-inclusive hybrid datasets (OBS+ERF+N) and non-ERF (OBS+N) datasets across 19 initial condition (IC) dates of 2021 rice crop season. During the early vegetative phase, particularly IC dates from 9 June to 30 June, the incorporation of ERF into the weather datasets did not lead to a consistent improvement in yield simulation performance. Correlation coefficients remained low to moderate ($r = 0.593$ on 16 June and $r = 0.659^{*}$ on 6 June). This reflects the limited predictive skill of ERF during early crop development, possibly due to high uncertainty in rainfall forecasts during this period and the less weather-sensitive nature of crop growth stages. However, beginning from 14 July, a notable improvement in performance was observed. The correlation between ERF-inclusive yield simulations and OBS-based simulations strengthened significantly ($r = 0.805^{**}$), 28 July ($r = 0.872^{**}$), 4 August ($r = 0.906^{**}$), 11 August ($r = 0.930^{**}$) and 18 August ($r = 0.926^{**}$) indicating that forecasts were beginning to capture relevant weather signals affecting crop development. During reproductive stage, the results indicated robust and consistent improvements in simulated yield prediction through ERF integration on all IC dates (25 August, 1, 8, and 15 September) with strong positive correlations between ERF-inclusive simulations and those driven by observed weather ($r = 0.965$ to 0.982 ; $p < 0.01$). ERF-omitted datasets also achieved high correlations ($r = 0.963$ to 0.963) (Fig.1c). During ripening phase with all IN dates (22 and 29 September; 6 and 13 October), both ERF-inclusive and ERF-omitted simulations displayed statistically significant positive correlations with the observed-weather-based yields (Fig. 1c). In general, correlation strengths between the two approaches were comparable, particularly during the early part of the ripening phase. However, as the crop neared physiological maturity, ERF-inclusive simulations consistently demonstrated improved alignment with the

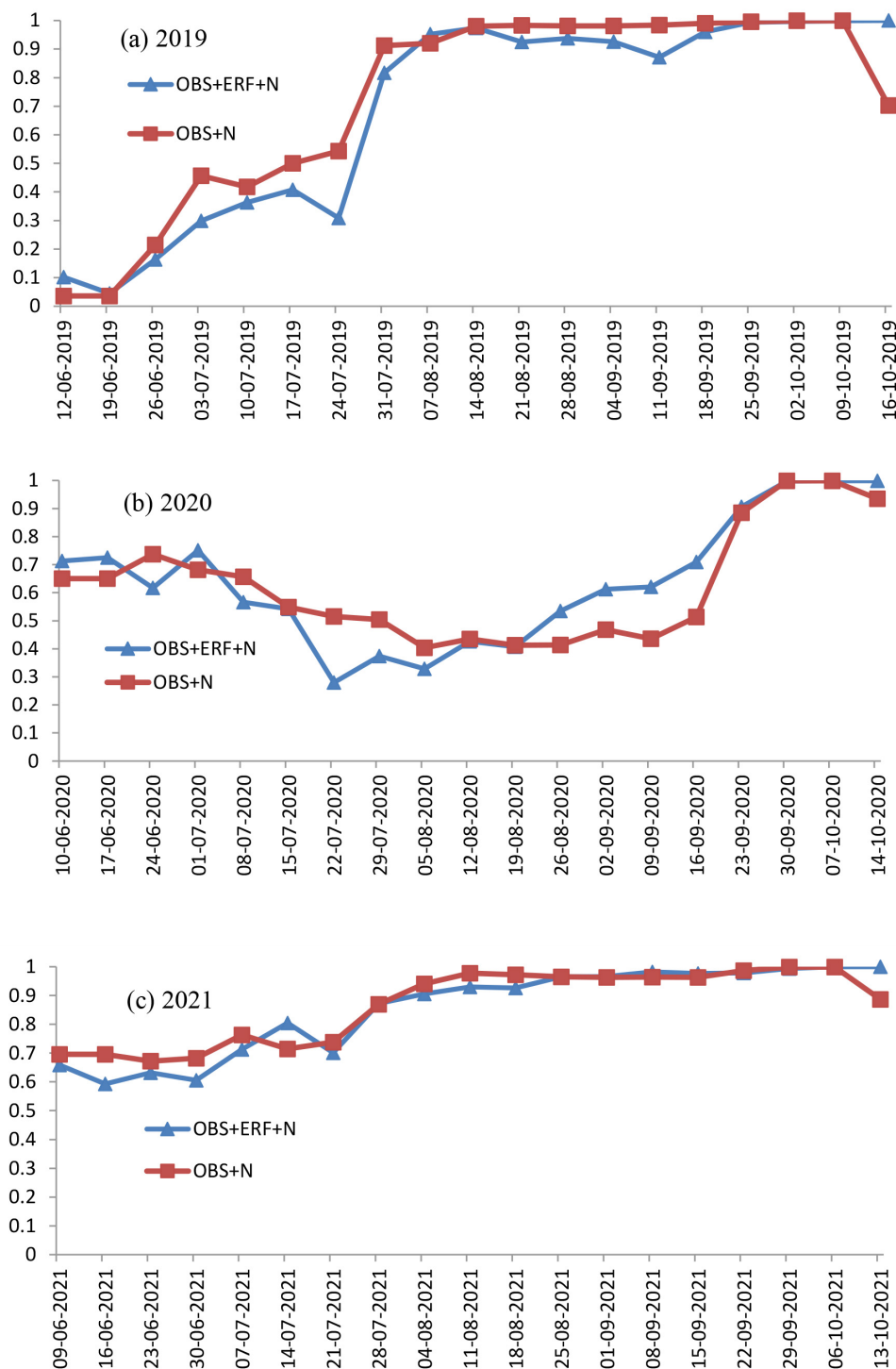


Fig. 1: Correlation coefficients of simulated yield obtained using OBS weather with simulated yield obtained using OBS+ERF+N and OBS+N weather datasets for (a) 2019, (b) 2020 and (c) 2021 under all IC dates.

benchmark yields.

Overall performance of ERF in simulating rice yield

To comprehensively assess the utility of the extended range forecast (ERF) system in enhancing rice yield simulations, a

phase-wise pooled analysis for three critical crop stages (vegetative, reproductive, and ripening) spanning the 2019 to 2021 *kharif* seasons are presented in Table 4. The results demonstrate that across all three seasons and crop phases, both ERF-inclusive and ERF-exclusive datasets showed statistically significant positive

Table 4: Simulated yield along with correlation (r) and RMSE of simulated yield obtained using observed weather with simulated yield obtained using ERF-inclusive and OBS+N weather datasets during three phases of the rice (pooled over IC).

Year	OBS Yield (kg ha ⁻¹)	OBS + ERF + Normal Yield (kg ha ⁻¹)	Correlation (r)	RMSE (kg ha ⁻¹)	OBS + Normal Yield (kg ha ⁻¹)	Correlation (r)	RMSE (kg ha ⁻¹)
Vegetative phase							
2019	3724.6	3448.7	0.461**	881.8	3362.3	0.499**	884.5
2020	3803.8	3740	0.408**	926.6	3793.3	0.463**	837.9
2021	3801.3	3433	0.626**	973.5	3506.1	0.754**	771.7
Reproductive phase							
2019	3724.6	3616	0.921**	367.5	3314.3	0.983**	449.5
2020	3803.8	4049.9	0.609**	775.9	3982.6	0.455**	852
2021	3801.3	4094	0.962**	424.6	3798.5	0.963**	295.2
Ripening phase							
2019	3724.6	3691.2	0.997**	80.4	3543.9	0.916**	393
2020	3803.8	3793.3	0.959**	212.2	3714.1	0.944**	257.8
2021	3801.3	3835.6	0.985**	193.4	3724.8	0.967**	285.6

** Correlation is significant at the 0.01 level (2-tailed). *Correlation is significant at the 0.05 level (2-tailed).

correlations with the OBS-based simulations ($p < 0.01$). During the vegetative phase, the performance of ERF-inclusive datasets was relatively modest. Correlation coefficients ranged between 0.408 and 0.626, with RMSE values between 881.8 and 973.5 kg ha⁻¹. Interestingly, in 2021, the ERF-excluded dataset exhibited a higher correlation ($r = 0.754^{**}$) and lower RMSE (771.7 kg ha⁻¹) than the ERF-inclusive counterpart ($r = 0.626^{**}$, RMSE = 973.5 kg ha⁻¹), suggesting limited predictive value of ERF during early crop development stages. This may be attributed to the dominance of antecedent soil moisture, sowing practices, and other non-weather factors during the vegetative phase, which are less influenced by medium-range forecasts.

The inclusion of ERF data led to a marked improvement in simulation performance during the reproductive phase. For instance, in 2021, the ERF-inclusive dataset achieved a high correlation ($r = 0.962^{**}$) and reduced RMSE (424.6 kg ha⁻¹), closely matching the performance of the ERF-excluded dataset ($r = 0.963^{**}$, RMSE = 295.2 kg ha⁻¹). The 2019 season showed a very strong correlation with OBS-based simulations ($r = 0.921^{**}$ for ERF-inclusive and $r = 0.983^{**}$ for ERF-excluded), though the RMSE was marginally lower for the ERF-inclusive scenario. These findings underscore the potential of ERF products in capturing intra-seasonal variability and episodic rainfall events critical to reproductive development, thereby improving simulation reliability (Table 4).

ERF's effectiveness peaked during the ripening phase, where its incorporation yielded the highest simulation accuracy. In 2019, the ERF-inclusive dataset achieved an exceptionally high correlation ($r = 0.997^{**}$) and a minimal RMSE of 80.4 kg ha⁻¹, significantly outperforming the ERF-excluded dataset ($r = 0.916^{**}$, RMSE = 393.0 kg ha⁻¹). Similar improvements were noted in 2020 and 2021, with RMSE reductions of 45.6 kg ha⁻¹ and 92.2 kg ha⁻¹, respectively, when ERF was incorporated. These results suggest that ERF is particularly effective in capturing late-season weather variability such as untimely rainfall or dry spells that substantially influence grain filling and final yield outcomes.

CONCLUSION

The effectiveness of the extended range forecast (ERF) system in simulating rice yield is most pronounced during the reproductive phase of crop development. In this critical mid-season stage, ERF-integrated weather datasets outperformed those constructed by appending observed weather with climatological normal. Unlike climatological averages, which fail to account for short-term atmospheric variability, ERF products capture transient, extreme, and intra-seasonal weather events—factors that have a substantial impact on yield formation. This enhanced ability to reflect real-time atmospheric dynamics results in yield simulations that more closely approximate observed field outcomes. These findings highlight the strategic value of incorporating ERF into crop simulation models such as DSSAT during the reproductive stage, when crops are highly sensitive to environmental stressors such as temperature spikes, rainfall variability, and humidity shifts. Timely and realistic simulations during this phase can significantly improve yield forecasting accuracy, supporting better-informed agricultural decision-making and early warning systems. In summary, ERF offers considerable promise in advancing weather-informed crop forecasting, particularly when applied during the reproductive phase. Continued investment in model calibration, real-time validation, and methodological enhancements will be essential to fully unlock its potential for climate-smart agriculture and risk-informed decision-making at regional and national scales.

ACKNOWLEDGEMENT

We gratefully acknowledge the Numerical Weather Prediction Division of the India Meteorological Department (IMD) for their support in providing the necessary data and for facilitating the successful execution of this research.

Source of funding: This research was carried as part of project Gramin Krishi Mausam Sewa (GKMS), Ministry of Earth Sciences.

Conflict of Interests: The authors have no conflicts of interest to declare.

Data availability: Gridded Weather data can be made available by request from IMD NDC portal, <https://dsp.imdpune.gov.in/>.

Author contribution: **Mehnaj T. A:** Conceptualization, Analysis work, Manuscript preparation; **Pattanaik, D.R:** Conceptualization, guidance, editing. **K.K. Singh:** Principal Investigator, project GKMS; **Goroshi, S.:** Idea expansion. **Manik, S.K.:** Idea expansion.

Disclaimer: The contents, opinions and views expressed in the research article published in the Journal of Agrometeorology are the views of the authors and do not necessarily reflect the views of the organizations they belong to.

Publisher's Note: The periodical remains neutral with regard to jurisdictional claims in published maps and institutional affiliations.

REFERENCES

- Chattopadhyay, N. (2023). Advances in application of sub-seasonal weather forecast in Indian agriculture. *J. Agrometeorol.*, 25(1): 34-41. <https://doi.org/10.54386/jam.v25i1.2047>
- GoI. (2024). "Agricultural Statistics at a Glance 2023". Ministry of Agriculture & Farmers Welfare Department of Agriculture, Cooperation & Farmers Welfare. Directorate of Economics and Statistics. pp.29.
- Harinarayanan M.N., Manivannan. V., Dheebakaran, Ga. and Guna. M. (2022). Usability of monthly ERFS (Extended Range Forecast System) to predict maize yield using DSSAT model over Erode District of Tamil Nadu. *J. Appl. Natural Sci.*, 14(SI): 244-250.
- IMD. (2014). "A manual for crop yield forecasting by statistical model". Agricultural Meteorology Division, India Meteorological Department, Shivajinagar, Pune. Ministry of Earth Sciences. pp.1.
- Pattanaik, D.R., Alone, A., Kumar, P. Phani, M, K., Mandal, Raju and Dey, Avijit. (2022). Extended-range forecast of monsoon at smaller spatial domains over India for application in agriculture. *Theor. Appl. Climatol.*, 147: 451-472.
- Sahai, A. K., Chattopadhyay, R., Joseph, S., Mandal, R., Dey, A., Abhilash, S., Krishna, R. P. M. and Borah, N. (2015). Real-time performance of a multi-model ensemble-based extended range forecast system in predicting the 2014 monsoon season based on NCEP-CFSv2. *Current Sci.*, 109(10): 1802-1813.
- Sahai, A.K., Sharmila, S., Abhilash, S., Chattopadhyay, R., Borah, N., Krishna, R.P.M., Joseph, S., Roxy, M., De, S., Pattnaik, S. and Pillai, P.A. (2013). Simulation and extended range prediction of monsoon intraseasonal oscillations in NCEP CFS/GFS version 2 framework. *Current Sci.*, 104(10):1394-1408.
- Sahu, V.N., Sahu, R.K. and Shrivastava, M.N. (1985). IR 36 for rainfed conditions in Madhya Pradesh, India. *Intern. Rice Res. Newsletter (Philippines)*. 10(5):6
- Singh, K.K., Baxla, A.K., Chaudhary, J.L., Kaushik, S. and Gupta, A. (2005). Exploring the possibility of second crop in Bastar Plateau region of Chhattisgarh using DSSAT crop simulation model. *J. Agrometeorol.*, 7(2):149-160. <https://doi.org/10.54386/jam.v7i2.834>
- Singh, P. (2023). Crop models for assessing impact and adaptation options under climate change. *J. Agrometeorol.*, 25(1): 18-33. <https://doi.org/10.54386/jam.v25i1.1969>